

Performance of EDLCs using Nafion and Nafion composites as electrolyte

C. K. Subramaniam · C. S. Ramya ·
K. Ramya

Received: 23 February 2010 / Accepted: 25 September 2010 / Published online: 11 October 2010
© Springer Science+Business Media B.V. 2010

Abstract We present the electrochemical performance of solid-state EDLCs constructed using composites of perfluorosulfonic acid polymer (Nafion) with micro porous polytetrafluoroethylene (PTFE) membrane and with cellulose acetate (CA), as electrolyte with carbon as electrodes (surface area: $260 \text{ m}^2 \text{ g}^{-1}$). The performance is compared with EDLCs constructed with perfluorosulfonic acid polymer as electrolyte. Scanning electron microscopy is used to study the morphology of the composite electrolyte while micro-Raman and IR measurements determine the integrity of the composite. The performance of the EDLC with perfluorosulfonic acid and PTFE composite electrolyte is good and comparable with the performance of the EDLC with pure perfluorosulfonic acid polymer electrolyte. A specific capacitance of 16 F g^{-1} is obtained for this EDLC with a maximum working potential of 2.0 V. There is an increase in the equivalent series resistance value from 0.08Ω for the Nafion EDLC to 4.1Ω for the Nafion/PTFE composite EDLC. However, the performance of the EDLC with the composite of Nafion/CA is poor due to substantial increase in ESR. The probable reasons are discussed.

Keywords Electric double layer capacitor · Electrochemical impedance spectroscopy · Perfluorosulfonic acid · Nafion composites · Micro-Raman · Charge–discharge

C. S. Ramya · K. Ramya
Centre for Fuel Cell Technology, ARC-International,
IITM Research Park, Taramani, Chennai,
Tamil Nadu 600113, India

C. K. Subramaniam (✉)
School of Advanced Sciences, VIT University, Vellore,
Tamil Nadu 632014, India
e-mail: cksupra@gmail.com

1 Introduction

Electrochemical double layer capacitors (EDLCs) have been recognized as an important and effective device for energy storage [1, 2]. The capacitance of the EDLCs arises from the separation of ionic charge at the interface between high specific area carbon electrodes and an aqueous or an organic electrolyte. The recent developments on the EDLCs are based on various carbon materials due to their structural integrity, chemical stabilities, and abundance. The main emphasis in the development of EDLCs is to develop carbon electrodes having high surface area [3]. This would enhance the storage density of the EDLC.

Various aqueous electrolyte solutions as well as organic electrolyte solutions have been used in conventional EDLCs. By replacing these liquid electrolytes with solid electrolytes like organic polymer electrolytes or inorganic silica gel electrolytes the reliability of the capacitors is expected to improve markedly [4]. Leakage of electrolytes can be avoided which normally leads to corrosion. The specific capacitance of the different carbon electrodes for the EDLCs assembled using various polymer electrolytes is shown in Fig. 1 [5–12]. It is evident that the specific capacitance is dependent on the carbon surface area and also the type of electrolyte used.

An alternative material that can be used in solid polymer EDLCs is the perfluorosulfonic acid polymer. This is available under the trade name Nafion from Du Pont. Several groups have investigated this polymer electrolyte for EDLC application [6–9, 13–16]. The perfluorosulfonic acid polymer possesses high ionic conductivity, good thermal stability, adequate mechanical strength, and excellent chemical stability. Staiti et al. [6] has reported that Nafion® is an ideal polymer electrolyte for an all-solid EDLC. They reported a specific capacitance of 13.2 F g^{-1}

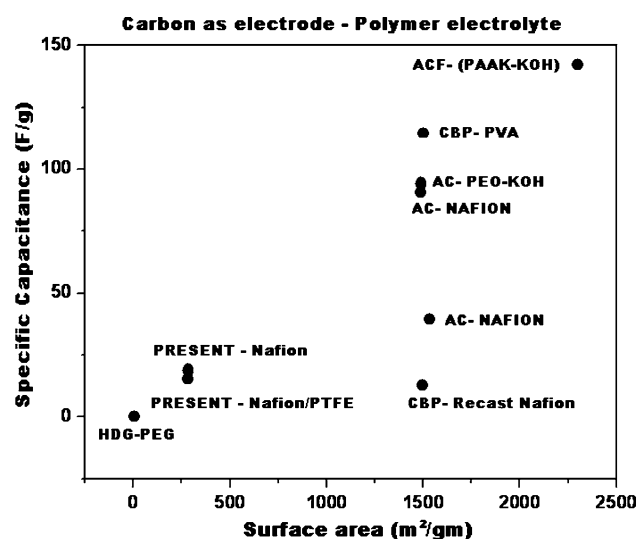


Fig. 1 Variation of specific capacitance with carbon surface area for systems using carbon as electrodes and polymers as electrolytes *HDG* High density graphite; *CBP* carbon black pearl; *AC* activated carbon; *PEO* poly ethylene oxide; *KOH* potassium hydroxide; *ACF* activated carbon fibre; *PVA* poly vinyl alcohol; *PAAK* potassium polyacrylate

for carbon Black Pearl 2000 (Cabot $1546 \text{ m}^2 \text{ g}^{-1}$ BET) as the active material. Recently, we have reported [17] a specific capacitance of 20 F g^{-1} for carbon–carbon EDLC using Nafion[®] as an electrolyte. However, the use of Nafion[®] [18] is not very economical for such applications.

Composite polymer electrolytes have been of interest due to their mechanical strength in the dry state and the dimensional stability in the hydrated state, handling ease, and availability of very thin sections. These composite polymer electrolytes have been tested for fuel cell applications. Liu et al. [19] have reported that the perfluorosulfonic acid/polytetrafluoroethylene (Nafion/PTFE) composite polymer have high mechanical strength and can be made into thinner sections as compared to the pure perfluorosulfonic acid polymer electrolyte.

In this article, an attempt was made to study the performance of perfluorosulfonic acid (Nafion)/polytetrafluoroethylene (expanded PTFE) composite polymer and perfluorosulfonic acid (Nafion)/Cellulose acetate (CA) composite polymer for EDLC application. We used two types of composite electrolyte based on the matrix–electrolyte structure. The CA composite was prepared using the CA matrix, which is hydrophilic and has macro pores. The PTFE composite was prepared using hydrophobic micro porous expanded PTFE matrix with an average pore size of $0.5 \mu\text{m}$.

The article presents a comparative study of the EDLC assembled using Nafion, Nafion/PTFE and Nafion/CA composite polymer electrolytes in the EDLC construction. The polymer used in the construction of the EDLC was maintained at room temperature without any external

hydration. The carbon used for the electrodes was the commercially available Vulcan XC 72 from Cabot with a typical surface area of $260 \text{ m}^2 \text{ g}^{-1}$. Scanning electron microscopy was used to study the morphology of the composite electrolyte while IR and Micro-Raman spectroscopy was used to determine the integrity of the composites. The EDLCs were studied using electrochemical impedance spectroscopy (EIS), cyclic voltammetry (CV) and charge–discharge profiles.

2 Experimental

2.1 Preparation of the composite polymer

2.1.1 Preparation of the Nafion/PTFE composite polymer

The preparation of the Nafion/PTFE composite polymer is given elsewhere [20].

2.1.2 Preparation of the Nafion/CA composite polymer

The composite was prepared using thin sections (typical thickness: 0.01 mm) of cellulose acetate of size 100 cm^2 . This section was soaked in 10 wt% perfluorosulfonic acid solutions for 60 s and dried in a vacuum oven at $70 \text{ }^\circ\text{C}$ for 1 h. The process was repeated a few times to obtain uniform composite.

2.2 Characterization of the polymer electrolyte

2.2.1 Scanning electron microscopy studies

A scanning electron microscope was used to investigate the morphology of surface and cross section of composite polymer electrolytes. The micrographs were recorded using Hitachi S-3400S instrument.

2.2.2 IR and Raman spectroscopic studies

The IR and Micro-Raman spectroscopic measurements were performed at room temperature on pure perfluorosulfonic acid polymer and perfluorosulfonic acid/PTFE composite polymer to ascertain polymer conformation, composition, and molecular orientation. The Micro-Raman Spectra is complementary to the IR spectra. This may provide micro structural information where no IR absorption takes place. Since the perfluorosulfonic acid/PTFE is a micro composite, in which the micropores of the PTFE have been filled with the perfluorosulfonic acid polymer; the Micro-Raman spectra could be useful in determining the integrity of the composite. IR spectroscopic measurements were performed using a Perkin-Elmer Spectrum1 FTIR

instrument. Raman measurements were conducted using a LabRam HR800 instrument.

2.3 Preparation of the electrode material

Vulcan XC 72 with a typical surface area of $260 \text{ m}^2 \text{ g}^{-1}$ and an average particle size of 30 nm was used as the raw material for the carbon electrodes. The electrode of size ($1 \times 10 \text{ cm}^2$) was prepared using solution of perfluorosulfonic acid as binder. The volume resistivity of the electrodes was found to be $3.63 \text{ m}\Omega \text{ cm}$ for an electrode thickness of 400 μm .

2.4 Assembly of the symmetric super capacitor single cell

The assembly of the EDLC is shown in Fig. 2. Two electrodes each of 10 cm^2 were assembled using pure perfluorosulfonic acid polymer Nafion[®], perfluorosulfonic acid/PTFE composite polymer (Nafion/PTFE) and perfluorosulfonic acid/Cellulose acetate composite polymer (Nafion/CA). The electrodes and the electrolyte were laminated at $130 \text{ }^\circ\text{C}$ for 60 s. This assembly was placed between two grafoil[®] sheets which was used as current terminals. Insulating gaskets were placed on both the internal faces of the end plates to prevent lateral shorting and to delimit the central capacitor portion and to seal the cell assembly.

2.5 Characterization of the assembled cells

The AC impedance spectroscopy measurements were performed in the frequency range: 100 kHz–10 mHz. Cyclic voltammetric measurements of the cell were made in the potential range -1 to 1 V under the potential scan rate of $1\text{--}100 \text{ mV s}^{-1}$. The capacitors were charged and discharged at constant current of $1\text{--}100 \text{ mA}$. All electrochemical measurements were performed at room

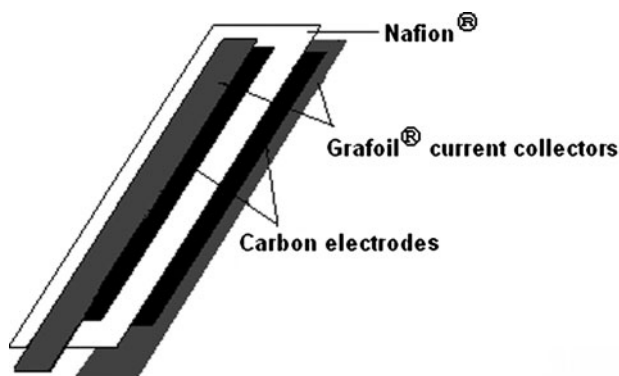


Fig. 2 EDLC assembly

temperature using an Autolab PGSTAT 30 potentiostat/Galvanostat with an inbuilt FRA.

3 Results and discussions

3.1 Scanning electron microscopy studies

Figure 3a and b shows the surface SEM micrograph of plain PTFE and CA polymer matrix, respectively. The PTFE polymer matrix contains micropores, which are uniformly distributed, whereas the CA matrix is randomly spread with larger pores or cavities. The size of the pores is of the order of $0.5 \mu\text{m}$. Figure 3c represents the surface micrograph of the Nafion/PTFE composite showing uniform distribution of Nafion polymer in the PTFE matrix, whereas Fig. 3d presents the surface micrograph of the Nafion/CA composite showing random distribution of the Nafion in the matrix. In the case of the Nafion/PTFE composite, the perfluorosulfonic acid solution penetrates through the micropores and fills them [20]. At very high magnification fissures on the surface of the membrane are seen. Figure 3e and f shows the SEM micrograph of the cross-section of Nafion/PTFE composite polymer and Nafion/CA composite polymer. The uniformity of the Nafion polymer distribution is evident.

3.2 IR and Raman spectroscopic studies

The IR spectroscopy and Micro-Raman spectroscopic were performed at room temperature on plain perfluorosulfonic acid polymer Nafion[®], plain PTFE and (Nafion/PTFE) composite polymer. This is presented in Fig. 4a and b, respectively. All the PTFE modes are observed in both IR and Micro-Raman spectra without any wave number shift (Fig. 4c). In addition, some signatures of the pendant chain, which are both IR and Raman active are also observed. In the Raman spectra, the band assignments for PTFE in the region $250\text{--}1250 \text{ cm}^{-1}$ correspond to CF_2 vibrations [21]. The low frequency bands at 290 and 390 cm^{-1} correspond to the twisting vibrations of the CF_2 . The bands at 730 and 1210 cm^{-1} corresponds to the symmetric and asymmetric stretching of the of the CF_2 molecule, respectively. The bands at 1290 and 1390 cm^{-1} correspond to the stretching vibrations of the C–C molecule [21].

The band assignments for the pure perfluorosulfonic acid polymer are similar to that of the PTFE. There are four additional bands at 390, 510, 975, and 1150 cm^{-1} . The characteristic functional groups C–O–C and SO_3 stretching vibrations of pure perfluorosulfonic acid polymer are found to be at 975 and 1150 cm^{-1} , respectively. The Raman spectra of Nafion/PTFE composite polymer

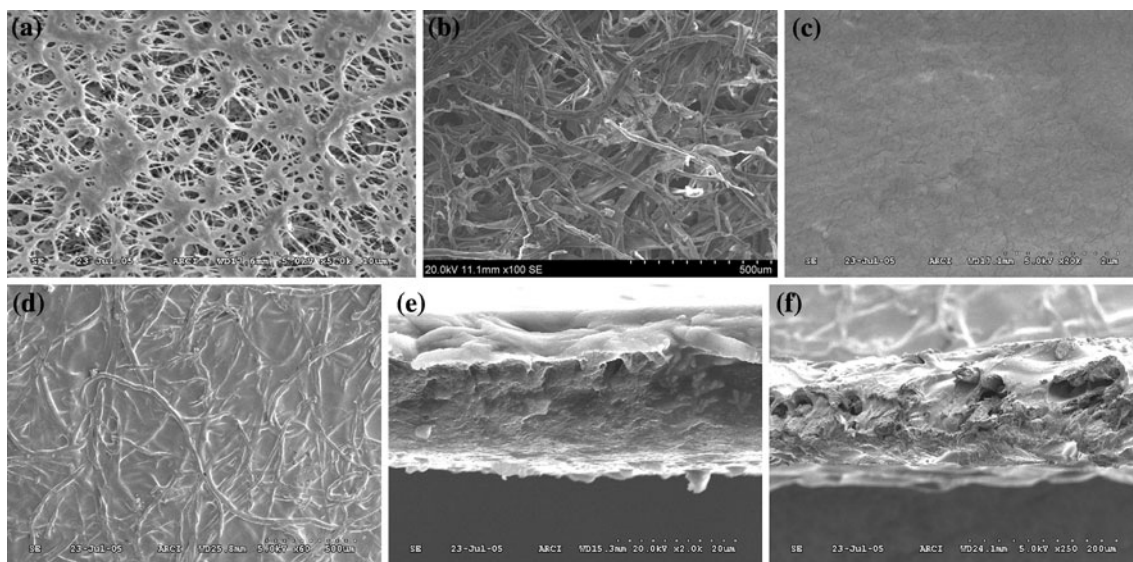


Fig. 3 SEM micrograph of the composite membranes **a** Surface PTFE polymer; **b** surface CA polymer, **c** surface Nafion/PTFE composite, **d** surface Nafion/CA composite, **e** cross-section Nafion/PTFE composite, **f** cross-section Nafion/CA composite

resemble the spectra of the plain PTFE polymer. The bands (indicated as asterisk in Fig. 4b) at 975 and 1150 cm^{-1} corresponding to C–O–C and SO_3 stretching vibrations found to be weakened in the Nafion/PTFE, composite.

The pores of the PTFE matrix are of the order of $0.5\ \mu\text{m}$. The Nafion model [21] suggests ionic clusters of the order of $3\text{--}5\ \text{nm}$ in diameter dispersed in a hydrophobic medium. Intrusions of the clusters into the fluorocarbon phase are also evident. As the average size of the ionic clusters is much smaller than the pore size of the matrix, the composite polymer electrolyte is similar to the Nafion polymer electrolyte. However, the extent of the PTFE matrix is much higher than the Nafion polymer cluster in the matrix. The clusters are joined by the tortuous path through the micropores. This results in higher resistance. The IR spectra of the Nafion/PTFE composite compared with that of the pure Nafion polymer shows slightly lower intensity for the $-\text{SO}_3\text{H}$ and the $-\text{C}-\text{O}-\text{C}-$ group. In the Raman spectra, the $-\text{SO}_3\text{H}$ peak is weakened due to higher intensity for the CF_2 group which occurs at 731 cm^{-1} . The $-\text{C}-\text{O}-\text{C}-$ group is totally embedded in the Raman spectra of the composite. The two spectra thus provide an insight into the effect of the environment on the ionic sites of the polymer electrolyte. As there is no shift in the wave number of the symmetric stretching vibration $-\text{SO}_3\text{H}$ group, the spectra suggests that the sulfonic acid clusters are only intercalated in the matrix, i.e., there are no interactions and the $-\text{SO}_3\text{H}$ groups are free for ion exchange. The same model may not be applicable for the Nafion/CA composite (Table 1).

3.3 Ac impedance measurements

The EIS measurement provides a correlation between the dependence of the capacitance with respect to the frequency [1]. Higher the frequency dependence of the EDLC, higher will be the power response. The Nyquist plots for the EDLC assembled with Nafion/PTFE composite polymer and Nafion/CA composite polymer as electrolyte is presented in Fig. 5. Equivalent series resistance (ESR) is an important quantity in evaluating the EDLC characteristics [22]. The effective ESR is revealed as the intercept on the Z' axis as $\omega \rightarrow \infty$ [1]. The impedance values are given in Table 2. The ESR value is found to be higher for the composite-based EDLCs.

In the impedance curves for Nafion/CA composite polymer, a depressed semicircle is observed. This is caused due to the heterogeneity of the EDLC, i.e., overlapping of several impedances due to the multiphase in the EDLC. On the other hand, a straight line is observed for Nafion/PTFE composite polymer in the frequency range studied indicating that internal resistance of the capacitor is smaller as compared to the EDLC with Nafion/CA composite polymer as electrolyte. Since the internal resistance is higher in this case, we focused only on the performance of the EDLCs using perfluorosulfonic acid/PTFE composite polymer as electrolyte.

The time constant (RC) of the EDLC is an important parameter and is characteristic of the EDLC assembly. The time constant values are calculated from the low frequency value of capacitance and the high frequency value of the ESR [23]. Estimated values of RC are found to be $4.8\ \text{s}$

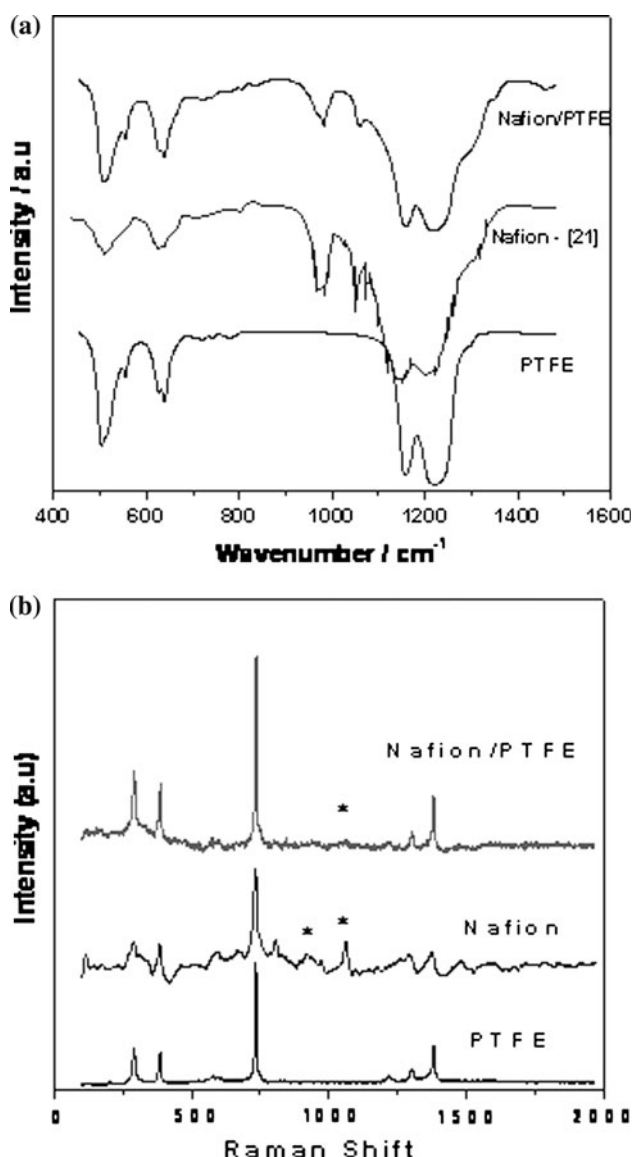


Fig. 4 a IR Spectra for a PTFE, b Nafion® and c Nafion/PTFE composite b Raman Spectra for a PTFE, b Nafion® and c Nafion/PTFE composite

for Nafion/PTFE-based EDLC and 1.25 s for plain Nafion-based EDLC. It shows that quick charge propagation takes place in this case.

Figure 6a shows Bode angle plot for the EDLCs based on Nafion polymer, Nafion/PTFE composite polymer, and Nafion/CA composite polymer. The circuit analysis is done using the Bode plot. The EIS data is fitted to an equivalent circuit as shown in Fig. 6b (inset), describing a series combination of a resistance and a constant phase element (CPE). A good fit was obtained with an error percentage of 0.5–0.8%. The constant phase element is introduced to explain the deviations of double layer capacitance from ideal behavior. If the CPE element value tends to 1.0, it resembles an ideal capacitor. If the value tends to 0.5,

Table 1 Characteristics Raman assignments for PTFE, Nafion and Nafion/PTFE composite

Wave length (λ/cm^{-1})			Assignment
Nafion®	PTFE	Nafion/PTFE	
290	290	290	t(CF ₂)
310	–	–	t(CF ₂)
390	390	390	t(CF ₂)
590	–	–	CF ₂ stretching
730	730	730	v _x (CF ₂)
975	–	–	C–O–C
1150	–	1150 (w)	SO ₃ stretching
1210	1210	–	v _{ax} (CF ₂)
1290	1290	1290 (w)	C–C stretching
1390	1390	1390 (w)	C–C stretching

it resembles the Warburg element. In this work, CPE values are 0.71 and 0.7 for Nafion and Nafion/PTFE based EDLCs, respectively. Hence, it represents a capacitive element with some in-homogeneity at the interface. The values of the constant phase element calculated from the Bode plot are presented in Table 2.

For the Nafion-based EDLC, the phase angle tending to 90° indicates that the EDLC functions like an ideal capacitor [24]. The phase angle is slightly lower for Nafion/PTFE composite polymer-based EDLC. This is due to the higher internal resistance. This may also be due to the surface morphology of the electrode–electrolyte interface. There may be an introduction of a surface roughness at the interface, evident from the SEM images. The Bode plot for the Nafion/CA polymer electrolyte clearly depicts the dominance of the resistive part. The phase angle tends nearly to zero, which indicates the dominant resistive component.

The amplitude of the total impedance versus frequency plot (Fig. 7) shows two slopes, one at high frequency region and the other at low frequency region. The high frequency region (50 kHz–50 Hz) has a slope of zero; the low frequency region (50–0.01 Hz) shows a slope of 0.65. This shows that there is a variation of capacitance with frequency. In the dynamic mode this variation has to be taken into consideration [25].

3.4 Cyclic voltammetry

The carbon behaviour can be understood basically by cyclic voltammetry (CV) measurements. Typical cyclic voltammograms for Nafion and Nafion/PTFE-based EDLCs are shown in Fig. 8. The voltammograms for various scan rates does not show peaks indicative of oxidation–reduction processes, and almost rectangular shapes similar to that of a typical capacitor have been observed in

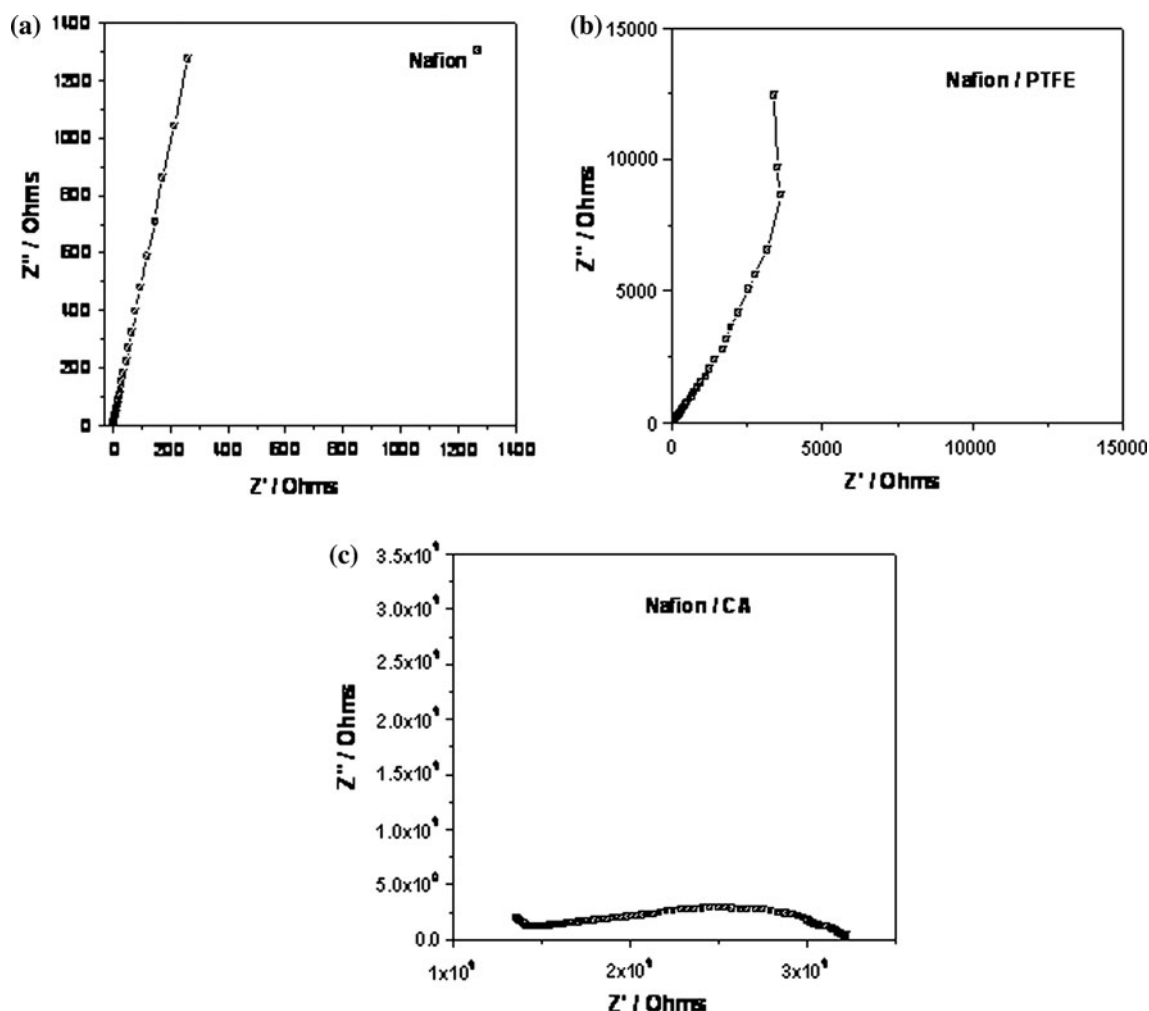


Fig. 5 Nyquist plots for the EDLC assembly with **a** Nafion[®], **b** Nafion PTFE and **c** Nafion/CA composite polymer electrolyte at room temperature

Table 2 Characteristics of the membrane and the EDLCs assembled using Nafion[®] and Nafion/PTFE composite polymer electrolyte

Membrane	Conductivity/S cm ⁻¹	Cell characteristics			
		From Nyquist plot		From Bode plot	
		ESR/Ω	Time constant/ms	ESR/Ω	CPE
Nafion	10 ⁻²	0.1	1.25	0.08	0.71
Nafion/PTFE	10 ⁻³	4.8	4.81	4.1	0.70

the working potential window. The voltammetric currents rapidly reach their plateau values for Nafion-based EDLC rather than for the EDLC with the Nafion/PTFE composite polymer. This indicates that the ESR of former is lower than that of latter [26].

The capacitance in Farads was calculated by using Eq. 1 [27],

$$C = I/s \dots \quad (1)$$

where I is the current, s is the scan rate.

High capacitance is observed at the lowest scan rate (1 mV s⁻¹). As the scan rate increases, the profiles gradually decrease. The results from Fig. 8 are tabulated in Table 3. The EDLC using solid electrolytes require lower scan rates for maximum charge accumulation, which has to match the inherent EDLC time constant. The decreasing trend in the capacitance suggests that the part of the surface of the carbon electrode for the accumulation of the charges is inaccessible at high charge/discharge rates. The specific capacitance, therefore obtained at lower scan rates is

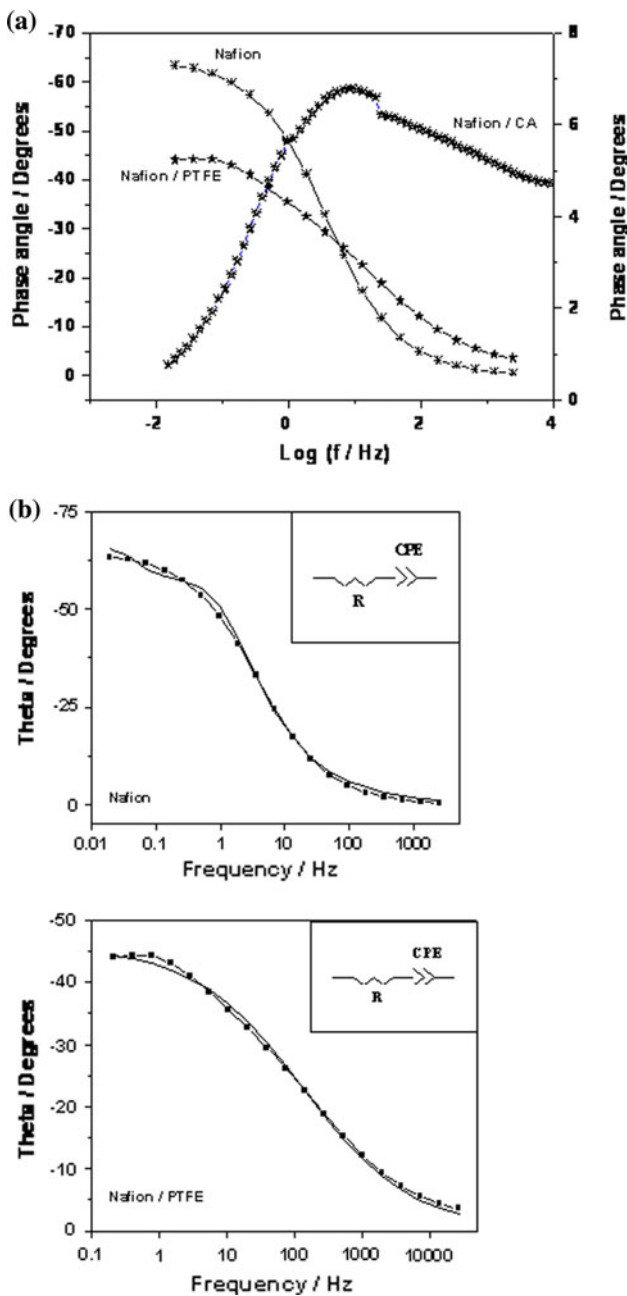


Fig. 6 a Bode plot for the EDLCs b Fitted Bode plot using Z—view software. The graph with *symbol* and the *line* indicates the experimental data and the *line graph* indicates the fitted curve for the corresponding experimental data. (*Inset*) Circuit description for the fitted data

believed to be close to the full utilization of the active carbon electrode.

The average value of capacitance is calculated from CV curves at 1 mV s^{-1} scan rate and are found to be 20 F g^{-1} for Nafion and Nafion/PTFE composite polymer electrolyte-based EDLCs. The EDLC assembled using Nafion/PTFE composite polymer electrolyte has a wider useful

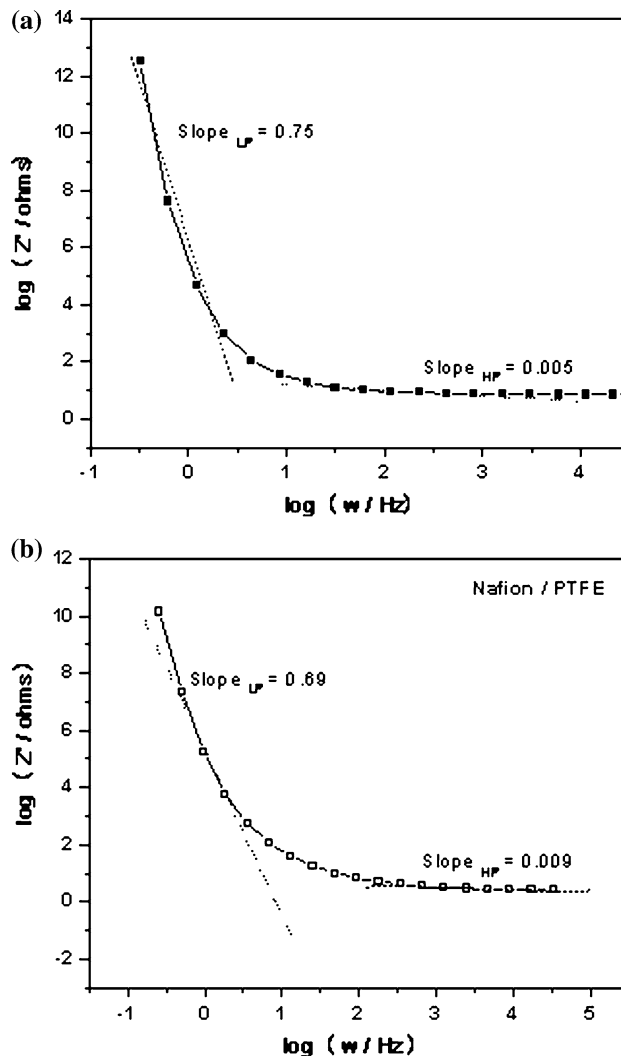


Fig. 7 Bode plot of total impedance versus frequency for the EDLCs; Different regions are shown with their slopes for a Nafion® and b Nafion/PTFE polymer electrolyte based EDLCs

potential window than the EDLC with the Nafion polymer. The potential window is limited by the Faradaic current in the EDLC using Nafion polymer. In the composite polymer electrolyte, the percentage of the ionic polymer Nafion is reduced by 60%. This may result in lesser ionic conducting site, i.e., SO_3^- groups, available at the interface for charge accumulation. However, this is not very evident in the performance. There is an increase in the ESR value from 0.08Ω for the Nafion EDLC to 4.1Ω for the Nafion/PTFE composite EDLC.

Figure 9 shows the typical cyclic voltammograms for Nafion and Nafion/PTFE composite polymer electrolyte-based EDLCs at 10 mV s^{-1} for ten cycles. An initial loss of capacitance of 20% for the first ten cycles is observed. The capacitance remains almost same for higher cycles, which indicates that the EDLC possesses good durability.

Fig. 8 Cyclic voltammograms for various scan rate *a* 1 mV s⁻¹, *b* 10 mV s⁻¹ and *d* 100 mV s⁻¹ for **a** Nafion[®] and **b** Nafion/PTFE polymer electrolyte based EDLCs

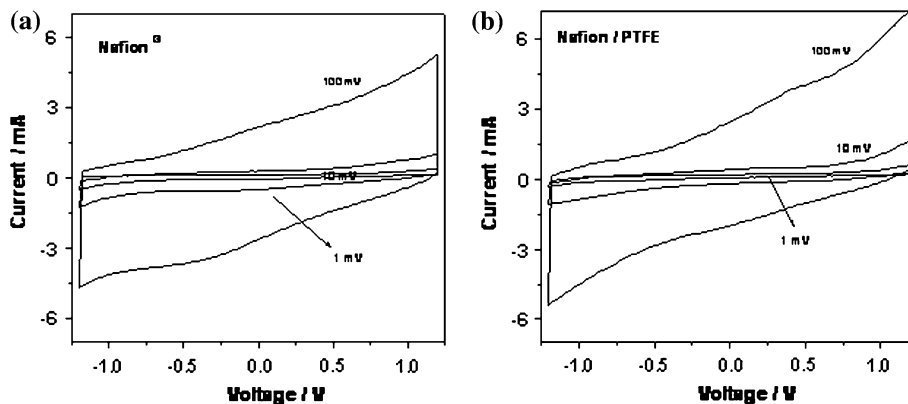


Table 3 Specific capacitance/(F g⁻¹) values for the EDLCs at various scan rates

Membrane	Scan rate/mVs ⁻¹		
	1	10	100
Nafion [®]	20	10.5	1
Nafion/PTFE	20	9	0.9

3.5 Charge/discharge characteristics

The charge/discharge profiles measured at the constant current of 1 mA for the EDLCs are presented in Fig. 10. The EDLC shows typical charge–discharge profile. The discharge profile of capacitors contains two parts; a resistive component, a sudden voltage drop (IR drop) represents the voltage change due to the internal resistance of the capacitor and the capacitive component which is related to the voltage change due to change in energy within the capacitor [28]. The IR drop is slightly higher for the Nafion/PTFE composite polymer electrolyte-based EDLC, which is evident from the high resistance of these EDLC, indicated in the EIS measurements. This factor has to be addressed in further EDLC developments. The capacitance can be calculated using the following equation,

$$C = It / V \dots \tag{2}$$

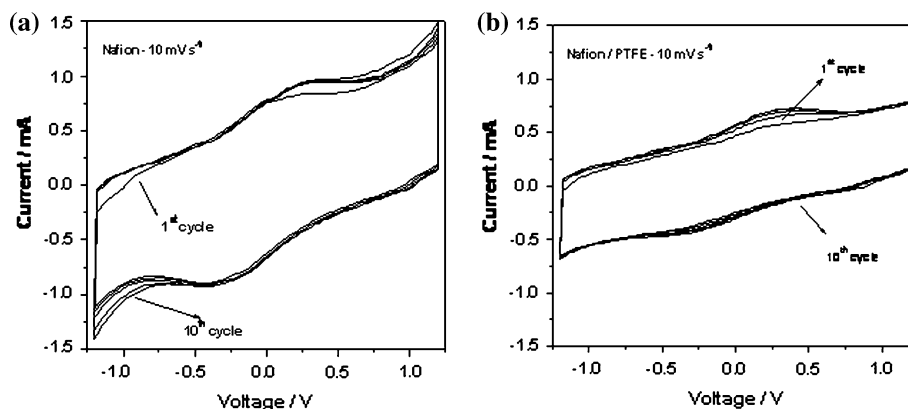
where *C*, *I*, *t*, and *V* are the capacitance, charge/discharge current, charge/discharge time and potential difference, respectively [4].

The capacitors have been subjected to charge/discharge cycling to the maximum working voltage of 2 V for more than 100 cycles. The charge/discharge profile of the EDLCs at a constant current of 100 mA for about 100 cycles has been shown in Fig. 11. The capacitance is almost constant over the period of cycles. There appears to be no visible drop even at higher number cycles for Nafion/PTFE composite polymer electrolyte-based EDLC.

4 Conclusions

The electrochemical performance of solid state EDLCs constructed using composites of Nafion with micro porous PTFE membrane as electrolyte with carbon as electrodes show good promise and an alternative to plain perfluoro-sulfonic acid polymer as electrolyte material. A specific capacitance of 16 F g⁻¹ is obtained for this EDLC, whereas it is 20 F g⁻¹ for the EDLC with plain perfluoro-sulfonic acid polymer electrolyte, with a maximum working potential of 2.0 V. The scanning electron

Fig. 9 Cycling performance of **a** Nafion[®] and **b** Nafion/PTFE composite polymer electrolyte-based EDLCs at a scan rate of 10 mV s⁻¹



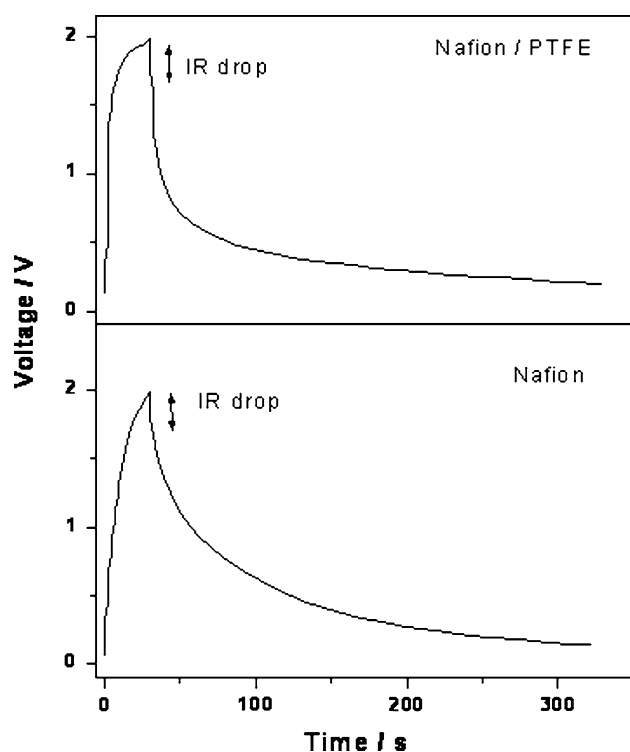


Fig. 10 Charge–discharge profile of the EDLCs at a constant current of 1 mA

microscopic results shows that the pores are well defined in the PTFE matrix indicating uniform distribution of proton sites and hence uniform charge distribution profiles, whereas in the case of the cellulose acetate matrix the distribution is random indicating a random distribution of the proton sites and hence affect the charge distribution profile. All the PTFE modes are observed in both IR and Micro-Raman spectra without any wave number shift. In the Micro-Raman measurements there is no shift in the wave number of the symmetric stretching vibration $-\text{SO}_3\text{H}$ group. The spectra suggests that the sulfonic acid clusters are only intercalated in the matrix, i.e., there are no interactions, and the $-\text{SO}_3\text{H}$ groups are free for ion exchange. The performance of the EDLC with the Nafion/PTFE composite was comparable with the performance of the EDLC with Nafion polymer electrolyte. There is an increase in the ESR value from 0.08Ω for the Nafion EDLC to 4.1Ω for the Nafion/PTFE composite EDLC. However, the performance of the EDLC with the composite of Nafion/CA was poor due to substantial increase in ESR. Further studies of the Nafion/PTFE composite have to be conducted to be able to use this electrolyte in solid EDLCs for commercial applications. Using Nafion/PTFE as an electrolyte will lead to fabrication of low cost EDLCs.

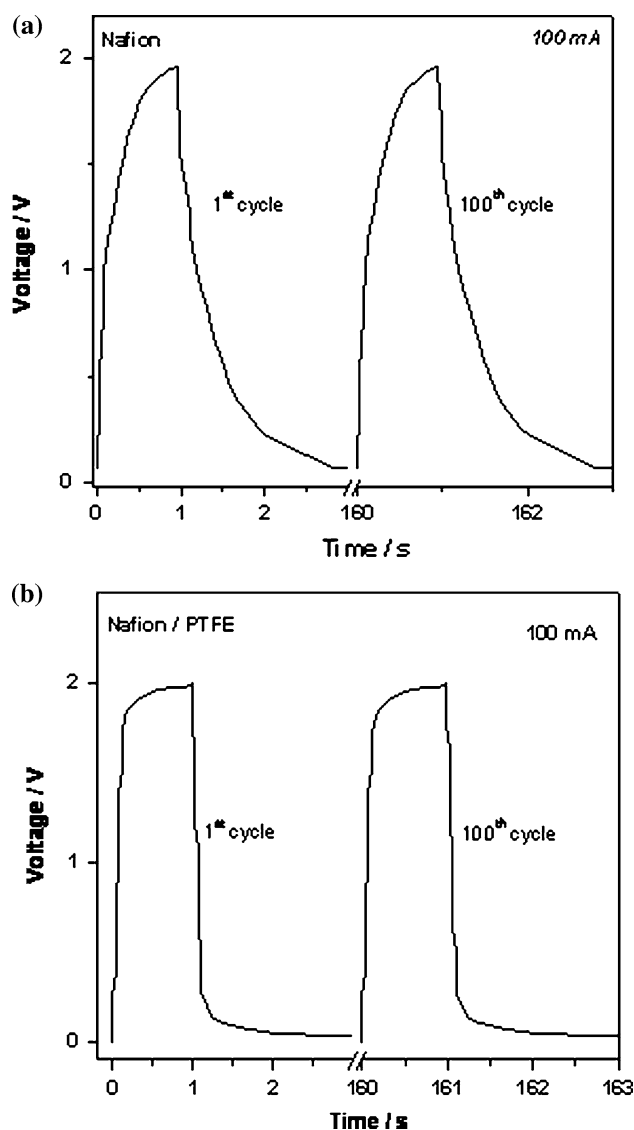


Fig. 11 **a** Charge–discharge profile for the 1st and the 100th cycle for the Nafion-based EDLC at a constant current of 100 mA **b** Charge–discharge profile for the 1st and the 100th cycle for the Nafion/PTFE-based EDLC at a constant current of 100 mA

Acknowledgments The authors would like to thank Dr. G. Sundarajan, Director, ARCI for supporting this work and Department of Science and Technology, Government of India, for financial support. The authors would like to thank Dr. K.S. Dhathathreyan CFCT-ARCI, for some useful insights and discussions. The authors would like to thank Dr. S. Kasivisvanathan, Department of Physics IIT Madras Chennai, India for the Micro-Raman spectroscopy and useful discussions regarding the spectra. Dr. C.S. Ramya would like to thank ARCI for a Post Doctoral Fellowship.

References

- Conway BE (1999) Electrochemical supercapacitors: scientific fundamentals and technological applications. Kluwer Academic/Plenum Publishers, New York

2. Hashmi SA, Upadhyaya HM (2002) *Solid State Ionics* 152–153:883–889
3. Kim T, Ham C, Rhee CK, Yoon SH, Tsuji M, Mochid I (2009) *Carbon* 47:226–233
4. Matsuda A, Honjo H, Hirata K, Tatsumisago M, Minami T (1999) *J Power Sources* 77:12–16
5. Mitra S, Shukla AK, Sampath S (2003) *Electrochem Solid State Lett* 6(8):A149–A153
6. Staiti P, Minutoli M, Lufrano F (2002) *Electrochim Acta* 47:2795–2800
7. Lufrano F, Staiti P (2004) *Electrochim Acta* 49:2683–2689
8. Staiti P, Lufrano F (2007) *Electrochim Acta* 53:710–719
9. Lufrano F, Staiti P (2004) *Electrochem Solid State Lett* 7(11):A447–A450
10. Lewandowski A, Zajder M, Frackowiak E, Beguin F (2001) *Electrochim Acta* 46:2777
11. Yang CC, Hsu ST, Chien WC (2005) *J Power Sources* 152:303–310
12. Iwakura C, Wada H, Nohara S, Furukawa N, Inoue H, Morita M (2003) *Electrochem Solid State Letters* 6:A37–A39
13. Lufrano F, Staiti P, Minutoli M (2003) *J Power Sources* 124:314–320
14. Pickup PG, Kean CL, Lefebvre MC, Guangchun L, Zhigang Q, Shan J (2000) *J New Mat Electrochem Systems* 3:21–26
15. Leela Mohana Reddy A, Estaline Amitha F, Imran Jafri S, Ramaprabhu S (2008) *Nanoscale Res Lett* 3:145–151
16. Park KW, Ahn HJ, Sung YE (2002) *J Power Sources* 109:500–506
17. Ramya CS, Subramaniam CK, Dhathathreyan KS (2010) *J Electrochem Soc* 157:A600–A605
18. Chen SL, Krishnan L, Srinivasan S, Benziger J, Bocarsly AB (2004) *J Membr Sci* 243:327–333
19. Liu F, Baolian Y, Xing D, Jingrong Y, Zhang H (2003) *J Membr Sci* 212:213–223
20. Ramya K, Velayutham G, Subramaniam CK, Rajalakshmi N, Dhathathreyan KS (2006) *J Power Sources* 160:10–17
21. Gruger A, Regis A, Schmatko T, Colomban P (2001) *Vib Spectrosc* 26:215–225
22. Chu A, Braatz P (2002) *J Power Sources* 112:236–246
23. Kierzek K, Frackowiak E, Lota G, Gryglewicz G, Machnikowski J (2004) *Electrochim Acta* 49:515–523
24. Niu C, Sichel EK, Hoch R, Moy D, Tennent H (1997) *Appl Phys Lett* 70(11):1480–1482
25. Mitra S, Lokesh KS, Sampath S (2008) *J Power Sources* 185:1544–1549
26. Hua CC, Wang CC, Feng-Chin W, Tseng RL (2007) *Electrochim Acta* 52:2498–2505
27. Lewandowski A, Galinski M, Krzyzanowski M (2003) *Solid State Ionics* 158:367–373
28. Michael MS, Prabaharan SRS (2004) *J Power Sources* 136:250–256